

Elsevier Editorial System(tm) for Journal of Electroanalytical Chemistry
Manuscript Draft

Manuscript Number:

Title: Irreversibility of catalytic reduction of dioxygen by dissolved hemin

Article Type: Regular Paper

Keywords: adsorption of reduced hemin at glassy carbon electrodes; catalytic current of dioxygen; non-linear relation of the catalytic current with concentration of dioxygen

Corresponding Author: Prof. Koichi Jeremiah Aoki, Ph.D.

Corresponding Author's Institution: University of Fukui

First Author: Koichi Jeremiah Aoki, Ph.D.

Order of Authors: Koichi Jeremiah Aoki, Ph.D.; Wenwen Li, MS; Jingyuan Chen, PhD; Toyohiko Nishiumi, PhD

Manuscript Region of Origin: JAPAN

Abstract: Hemin in aerated dimethylsulfoxide catalyzes the reduction of dioxygen at glassy carbon electrodes with a gain voltage for the catalysis, 0.5 V. The catalytic rate, observed as the reduction current, increases with an increase in concentrations of dioxygen, but reaches a maximum at 6% of the saturated concentration. The voltammetric peak current has a linear relation with the scan rate. These variations are different from the ordinary catalytic mechanism, in which hemin oxidized by dioxygen might be reused for the electrochemical reduction. The voltammetric peak current in deaerated hemin solution is diffusion controlled, whereas that in aerated solution is represented as a sum of the diffusion current and a surface wave. The catalytic current is caused by hemin incorporated with dioxygen, of which adsorption density is close to an amount of a monolayer. Therefore hemin films are not suitable for continuous reduction of dioxygen. Once the adsorbed layer is electrochemically oxidized to remove the adsorption film, the catalytic reduction wave is retrieved.

Suggested Reviewers: William R Heineman PhD
professor, Chemistry, University of Cincinnati
william.heineman@uc.edu
He is a pioneer for the reaction of hemin with dioxygen.

Zhen-Xing Liang PhD
professor, Chemistry and Chemical Engineering, South China University of Technology, Guangzhou
zliang@scut.edu.cn
His major is electrocatalysis by heat-treated hemin.

Rongzhong Jiang PhD
a group leader, US Army Research Laboratory
Rongzhong.jiang.civ@mail.mil
He is an active researcher of catalysis of dioxygen at modified electrodes for fuel cells.

Federica Valentini PhD

professor, Science & Techological Chemistry, Universita degli Studi di Roma Tor Vergata
federica.valentini@uniroma2.it

He works on catalysis of H_2O_2 at GC electrodes modified with hemin-carbon nanomaterial films.

Shiyun Ai PhD

professor, Chemistry and Material Science, Shandong Agricultural Universit

ashy@sdau.edu.cn

He works on electrocatalysis at hemin-modified graphite felt.

Dear an editor of Journal of Electroanalytical Chemistry:

I would like to submit the attached files to JEC as a full paper.

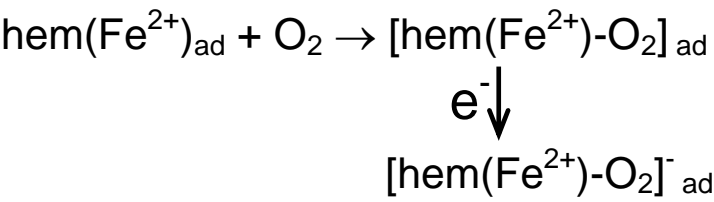
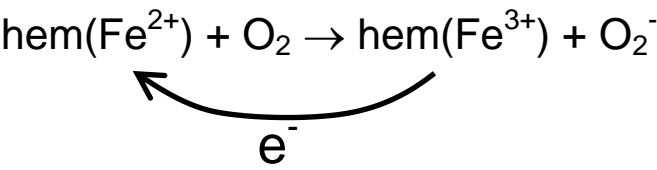
All the authors have agreed on the publication.

This manuscript aims at finding whether the catalytic reaction of dioxygen by hemin has a type of Fenton reaction or not.

The answer is no. Consequently the reaction cannot be used for an alternative of platinum cathodes for fuel cells.

Koichi J. Aoki

September 18, 2013



Which reaction occurs?

Hemin catalyzes reduction of O₂ at glassy carbon electrodes.

The catalytic current belongs to a surface process rather than volume reactions.

The current is not under the steady state.

It varies with concentrations of O₂ in a very narrow domain.

Irreversibility of catalytic reduction of dioxygen by dissolved hemin

Koichi Jeremiah Aoki^{*}, Wenwen Li, Jingyuan Chen, Toyohiko Nishiumi

*Department of Applied Physics, University of Fukui, Bunkyo 3-9-1, Fukui, 910-8507
Japan*

Abstract

Hemin in aerated dimethylsulfoxide catalyzes the reduction of dioxygen at glassy carbon electrodes with a gain voltage for the catalysis, 0.5 V. The catalytic rate, observed as the reduction current, increases with an increase in concentrations of dioxygen, but reaches a maximum at 6% of the saturated concentration. The voltammetric peak current has a linear relation with the scan rate. These variations are different from the ordinary catalytic mechanism, in which hemin oxidized by dioxygen might be reused for the electrochemical reduction. The voltammetric peak current in *deaerated* hemin solution is diffusion controlled, whereas that in *aerated* solution is represented as a sum of the diffusion current and a surface wave. The catalytic current is caused by hemin incorporated with dioxygen, of which adsorption density is close to an amount of a monolayer. Therefore hemin films are not suitable for continuous reduction of dioxygen. Once the adsorbed layer is electrochemically oxidized to remove the adsorption film, the catalytic reduction wave is retrieved.

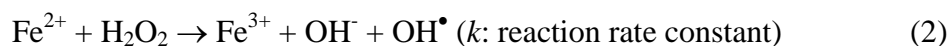
keywords: adsorption of reduced hemin at glassy carbon electrodes; catalytic current of dioxygen; non-linear relation of the catalytic current with concentration of dioxygen

^{*} Corresponding author, Fax: +81 776 27 8750, Email: kaoki@u-fukui.ac.jp (K.J. Aoki)

1. Introduction

Cobalt phthalocyanine has been demonstrated to work as electrocatalysis of the oxygen reduction reaction (ORR) in alkaline media by Jasinski for the first time [1]. Since then, the catalytic activity of metal porphyrins has been explored as alternatives of non-precious metal catalysts for ORR. Especially hemin, a natural porphyrinatoiron complex, has been able to reduce catalytically dioxygen and hydrogen peroxide at carbon paste electrodes [2-4]. Hemin-modified carbon fiber electrodes can also reduce dioxygen to water and hydrogen peroxide, depending on solvents [5]. The number of electrons transferred at hemin-coated glassy carbon electrodes varies with pH; a one-step four-electron reduction at $\text{pH} < 11$ and two successive steps at $\text{pH} > 12$ [6]. Heat treatment of hemin-modified carbon electrodes has enhanced the catalytic efficiency of ORR, similar to that of platinum electrodes [7]. Functional groups on the porphyrin periphery play a specific role in the electrocatalytic ORR, reportedly [8]. Catalytic performance has been improved by use of hemin/graphite felt composite electrodes [9], by immobilization of hemin on chemically converted graphene [10] and carbon nanotubes [11-13], by electrostatic binding of hemin on latex particles [14], by enhancing porosity of adsorbed layers [15,16], by heating the hemin-modified electrodes [7,17-19], and by immobilization of hemin into proteins [20]. Catalytic activity of hemin has been found for reductions of nitric monoxide [21,22], mercuric ion [23], antimalarial drug [24], nitrite [12,13], and hydroquinone [25].

The well-known electrochemical, catalytic reaction is exemplified by the Fenton reaction, in which electrochemically generated ferrous ion is oxidized to ferric ion by hydrogen peroxide [26], i.e.



Expressions for the catalytic current by linear sweep voltammetry have been derived on

the assumption of the mixed control of reaction (2) with diffusion of the soluble species [27]. The catalytic current at a large value of the reaction rate $k[\text{Fe}^{2+}][\text{H}_2\text{O}_2]$ is independent of scan rates, v , and is controlled by diffusion of H_2O_2 . In contrast, the current at a very small value of the rate is proportional to $v^{1/2}$. As a result, the current varies generally with v^p for $0 < p < 0.5$. This relation is, however, different from the voltammetric results ($p > 0.5$) of reduction of dioxygen with hemin although the model of reactions (1) and (2) has been applied to the analysis [4,6,8,9]. The other available model is the catalytic reaction of soluble species with the redox species adsorbed on an electrode [28]. This has not been applied to experimental results of hemin, to our knowledge, probably because application of the theoretical expressions needs detailed dependence on concentrations and scan rates. Another model used is for the preceding reaction at a rotating disk electrode [10,15,17]. It is obviously not suitable for explanations of the catalytic reaction.

The catalysis of dioxygen by hemin can be applied to fuel cells if current flows under the steady state in dioxygen-rich solutions. The steady-state currents have been observed at rotating disk electrodes [6,10,15,17]. It is not clear, however, whether the currents are a purely catalytic component or include the direct reaction by hydrodynamic transport of dioxygen. In order to discern the catalytic component from the direct mass transport reactions, it is necessary select conditions under which the reduction potential of hemin is much more positive than that of dioxygen. One technique is to use dimethylsulfoxide (DMSO) in which the potential difference is over 0.4 V [29]. Then we may examine time-variation of the catalytic currents in details. This report deals with time-dependence of the catalytic currents of dioxygen by hemin in DMSO, varying concentrations of dioxygen and hemin. The catalytic current will be demonstrated to be a non-steady-state by adsorption process [30,31].

2. Experimental

All the chemicals were of analytical grade. Hemin (Wako) with nominal 97 % purity was stored in a refrigerator. It was weighed after it became at a room temperature in order to avoid mixing with water. DMSO was distilled under reduced pressure and dried by means of molecular sieves.

A potentiostat used was Compactstat (Ivium, Netherlands). All electrochemical experiments were performed in a three-electrode cell including a Pt wire auxiliary electrode, a Ag/Ag⁺(0.01 M (= mol dm⁻³) AgNO₃) reference electrode and a working electrode. The working electrodes were the glassy carbon electrode 3 mm in diameter, the platinum disk electrode 1.6 mm in diameter and the gold disk electrode 1.6 mm in diameter. They were commercial available (BAS, Tokyo). A small disk platinum electrode, 0.1 mm in diameter, was home-made, coated with glass.

Spectro-electrochemical measurements was made with V-570 UV/VIS/NIR Spectrophotometer (Jasco, Japan). The spectro-electrochemical cell had a thin layer cell made of quartz 0.47 mm thick, into which the Pt mesh 0.076×50×10 mm³ with the density 80 lines per inch was inserted.

3. Results and Discussion

3.1 Reaction model of dissolved hemin

The voltammogram in hemin-included deaerated DMSO solution showed waves of a redox couple approximately at -0.7 V in Fig. 1(a). The other couple at -1.7 V (not shown here) is not related with the present discussion. Since the cathodic and the anodic peak currents were proportional to concentrations of hemin less than 3 mM, the wave should be caused by the reduction of hemin. The voltammograms did not vary with

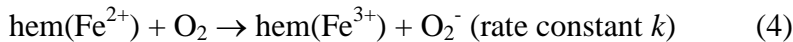
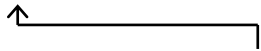
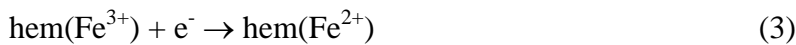
iterative scans. The cathodic peak current was proportional to the square roots of scan rates, ν , as shown in Fig. 2(a), and hence it should be controlled by diffusion of hemin. Concentration of electroactive hemin is smaller than that prepared by weight [32]. In order to determine the concentration accurately, we applied the method of the combinational use of a small disk electrode (0.1 mm in diameter) and a regular sized disk electrode (1.6 mm in diameter) [32]. This technique allows us to determine concentrations without knowing a value of the diffusion coefficient. The reduction peak currents at the 1.6 mm electrode were proportional to $\nu^{1/2}$ for $0.01 < \nu < 0.2 \text{ V s}^{-1}$. In contrast, those at the 0.1 mm electrode showed a linear relation with $\nu^{1/2}$ with an intercept. Taking the ratio of the slope of the former plot to the intercept of the latter plot [32], we evaluated the concentration to be 0.40 mM, which was smaller than that estimated from the weight (0.6 mM). The diffusion coefficient was evaluated to be $3.3 \times 10^{-6} \text{ cm}^2 \text{ s}^{-1}$ in DMSO.

When the hemin solution contained air, three cathodic waves appeared at -0.70 V, -0.9 V and -1.20 V, as shown in Fig. 1(b). The current at the first wave was by 1.5 times larger than the reduction peak of hemin, at the cost of the corresponding anodic current. The voltammogram in the aerated solution without hemin had no wave at -0.7 V or -0.9 V but showed the reduction wave at -1.2 V. The wave at -1.2 V can be ascribed to the reduction of dioxygen because the current was proportional to concentrations of dioxygen, as will be shown later. The enhancement of reduction peaks at -0.7 V and -0.9 V should be the catalytic current of dioxygen by hemin. The energetic gain of the catalysis is 0.5 V ($= -0.7 - (-1.2)$) or 48 kJ mol^{-1} , close to the bibliographic value [29]. The anodic wave at 0.2 V appeared in the aerated hemin solution when the potential was reversed at either -0.8 V or -1.0 V. Therefore it should be due to the products of the catalytic reactions.

In order to identify the species relevant to the catalytic reaction, we made spectro-electrochemical measurements at the platinum mesh electrode. Figure 3 shows

UV-spectra of (a) deaerated hemin solution when hemin, denoted by $\text{hem}(\text{Fe}^{3+})$, was electrochemically reduced to $\text{hem}(\text{Fe}^{2+})$ at the mesh electrode. The Soret bands appeared at 404 nm and 424 nm for (a) $\text{hem}(\text{Fe}^{3+})$ and (b) $\text{hem}(\text{Fe}^{2+})$, respectively, as are consistent with documented data [29,33-37]. When the hemin solution contained dioxygen (c), the band at 424 increased at the expense of the band at 404 nm. Therefore the reduced hemin should be responsible for the catalysis of dioxygen.

The time-variations of the absorbance are shown in Fig. 4 at (A) 404 nm and (B) 424 nm. The concentration of $\text{hem}(\text{Fe}^{3+})$ (at 404 nm) in the deaerated solution decreased with the time of the electrochemical reduction (circles) to generate $\text{hem}(\text{Fe}^{2+})$ (424 nm). When dioxygen is present, $\text{hem}(\text{Fe}^{3+})$ is reproduced with dioxygen by the amount of the concentration of the bold arrow in Fig. 4(A) (triangles), at the cost of $\text{hem}(\text{Fe}^{2+})$ in Fig. 4(B). These variations have reminded electrochemists [4,6,8,9] of the Fenton model of reaction (1) and (2), i.e.



On the assumption that $\text{hem}(\text{Fe}^{3+})$ would be generated at the first order reaction rate, we plotted logarithms of the normalized concentration of $\text{hem}(\text{Fe}^{3+})$, i.e. $A(\text{aerated})/A(\text{deaerated})$ at 404 nm, against the time in Fig. 4(A) on the right ordinate. The plot fell on a line, suggesting the first order reaction with respect to $\text{hem}(\text{Fe}^{3+})$. The value of the slope was 0.0023 s^{-1} . Since the reaction rate is expressed by $k[\text{hem}(\text{Fe}^{3+})][\text{O}_2]$, the value of the rate constant k is $9.2 \text{ M}^{-1} \text{ s}^{-1}$ for the concentration (0.5 mM) of the air-saturated dissolved dioxygen at 1 atm. The half-life of the reaction is 5 min ($= \ln(2)/0.0023 \text{ s}^{-1}$). This is too long for the time scale (a few seconds) of the present catalytic voltammetry.

In order to solve this contradiction, we examined the dependence of the current on the scan rates and concentrations of hemin and dioxygen in detail. Figure 2(b) shows the

plot of the catalytic peak current at ca. -0.7 V against $v^{1/2}$. If the catalytic reaction occurs according to mechanism (3) and (4), the current at very slow scan rates must be independent of the voltammetric time or v . Quantitatively, the steady-state current density is represented by $Fc^*(kD[\text{O}_2])^{1/2}$ for the diffusion coefficient D of hem(Fe^{2+}) and its bulk concentration c^* [27]. On the other hands, the catalytic current at high scan rates should be proportional to $v^{1/2}$ [27]. The plot in Fig. 2(b) is opposite to the prediction.

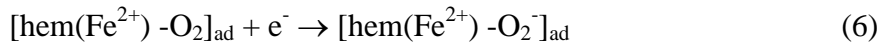
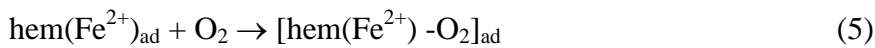
We changed the concentration of dioxygen by mixing three aliquots at adequate volume ratios; the deaerated, the air-saturated and the dioxygen-saturated hemin solutions. Figure 5 shows variation of the catalytic currents with the concentration ratios to the dioxygen-saturated solution at a given concentration of hemin. The current did not vary with the concentrations less than 0.03 of the dioxygen-saturated concentration (line (a)). The invariance indicates that the current should be controlled by the concentration of hemin. The current at the concentration ratio ranging from 0.03 to 0.06 varied proportionally to the concentration ratio (line (b)). It reached -6.5 μA for the ratio over 0.06. These variations are different from the conventional catalytic current which increases with an increase in concentration of catalyzed species (dioxygen) [27,38] even for the second order reaction [39]. Figure 6 shows plots of the catalytic peak currents against concentrations of hemin in the air-saturated solution. The current without dioxygen is proportional to hemin concentration (a), whereas that with dioxygen increases linearly with the concentration (b) as if the catalysis might occur even at $[\text{hemin}] = 0$, as shown at the intercept of the dashed line.

We made iterative voltammetric runs, between which dioxygen gas was bubbled in the solution. Figure 7 shows dependence of the peak currents (a-c) at -0.7 V for the catalytic current and of those (d) at -1.2 V for the reduction of dioxygen without hemin on the time of the bubbling. The reduction current of dioxygen without hemin increased with the time and reached the saturated value at 900 s, as is in accord with the conventional deaeration process. When solution contained hemin, the catalytic current

increased with the time in the same manner as the increase without hemin before 150 s bubbling. The catalytic currents were saturated to values corresponding to low concentrations of dioxygen. These variations are consistent with those in Fig. 5 and 6.

3.2 Reaction Model for adsorbed hemin

The scan rate-dependence of the catalytic currents in Fig. 2(b) seems to resemble the general adsorption behavior in that the peak currents deviate upward from the line which is proportional to $\nu^{1/2}$ at fast scans. When the peak currents were plotted against ν , they fell on a line in Fig. 8 (a), but showed an intercept. Therefore the current does not belong to a surface wave. If the catalytic component is superimposed on the diffusion current, the total current should be expressed by $I_p = k_1\nu^{1/2} + k_2\nu$ for constants k_1 and k_2 [28]. The plot of $\Delta I_p = I_p - k_1\nu^{1/2}$ against ν showed proportionality in Fig. 8(b). If the peak current density of the surface wave is caused by the simple adsorption with the form of $(F^2/RT)\Gamma\nu$ [40], the amount of the adsorbed species, Γ , is calculated to be 5×10^{-9} mol cm $^{-2}$ on the assumption of a one-electron transfer reaction. This value is close to the accepted values of the monolayer adsorption as well as reported values of adsorbed hemin [12,41,42]. The monolayer adsorption infers that the catalysis of O $_2$ should occur only by the absorbed amount without supply of O $_2$ by diffusion. Therefore, a possible mechanism of the catalytic current is



Reaction (5) represents the uptake of dioxygen in the adsorbed layer, while (6) includes the electron transfer reaction corresponding either to the wave at -0.7 V or -0.9 V. If $[\text{hem(Fe}^{2+}\text{)} - \text{O}_2^-]_{\text{ad}}$ was decomposed into $\text{hem(Fe}^{2+}\text{)}_{\text{ad}}$ and soluble O $_2^-$ or its stabilized species, dioxygen in solution would be catalyzed one after another through reaction (5) with the help of diffusional supply of dioxygen. Continuous catalysis requires the

reproduction of $\text{hem}(\text{Fe}^{2+})_{\text{ad}}$.

Adsorption depends generally on materials of substrates. Platinum and gold disk electrodes were used for the reduction of hemin instead of the glassy carbon. The reduction current densities of deaerated hemin solution at the Pt and the Au electrodes were almost the same as those at the GC electrode. They were also the same as in the aerated hemin solution. Consequently, the catalytic current can be observed only at the GC electrode. The formation of $\text{hem}(\text{Fe}^{2+})_{\text{ad}}$ seems to be restricted on carbon electrodes. The non-observation of catalytic current at the Pt and the Au electrodes is consistent with the slow reaction rate constant (5 min half-life) of the catalytic reaction estimated from the UV absorbance.

If $\text{hem}(\text{Fe}^{2+})_{\text{ad}}\text{-O}_2^-$ can be removed electrochemically from the electrode, a potential control is expected to continue the catalytic reaction intermittently. When the potential was cycled in the domain from -0.8 to 0.0 V in aerated hemin solution, the catalytic current decreased with the number of the scans, as shown in Fig. 9(c, d). The voltammograms cycled in the domain from -0.8 V to 0.6 V did not vary with the number of scans (Fig. 9 a, b). The invariance to the number of scans indicates that the anodic wave at 0.3 V should work as the removal of the adsorbed species. So far as potential is cycled between -0.8 V and 0.3 V, the dioxygen can be catalyzed intermittently. The catalytic reaction is, however, not under the steady state.

Of interest is catalytic current of dioxygen by hemin in aqueous solution. Since hemin is not dissolved in aqueous solution, water was added to the DMSO solution including 0.4 mM hemin so that water concentration was a few mM. The addition of water had no influence on the voltammograms. Therefore reactions (4) and (5) are valid in the presence of small amount of water.

4. Conclusions

Hemin can catalyze dioxygen in the form of an adsorbed adduct of hemin with dioxygen at glassy carbon electrodes. Since soluble hem(Fe^{2+}) is not reproduced from the adsorbed adduct, the catalytic reaction does not belong to the Fenton reaction. The catalytic current cannot keep a steady state even if dioxygen is supplied to the electrode by diffusion or convection. Since the adsorbed species is dissolved at the oxidation at 0.3 V, the electrode surface is renewed sufficiently for the catalytic reaction. In order to continue the catalytic reaction, it is necessary to remove the adsorbed species. Otherwise, the catalytic current is blocked gradually. Consequently, the catalysis of dioxygen by hemin is not suitable for an alternative to precious metals in fuel cells.

5. Acknowledgement

This work was financially supported by Grants-in-Aid for Scientific Research (Grants 25420920) from the Ministry of Education in Japan.

References

- [1] R. Jasinski, *Nature* 201 (1964) 1212-1213.
- [2] M. Brezina, *Ber. Bunsen Gesel.* 77 (1973) 849-852.
- [3] M. Brezina, A. H.-Matejkova, *Collect. Czech. Chem. Commun.* 38 (1973) 3024-3031.
- [4] N. Zheng, Y. Zeng, P.G. Osborne, Y. Li, W. Chang, Z. Wang, *J. Appl. Electrochem.* 32 (2002) 129-133.
- [5] S. Antoniadou, A.D. Jannakoudakis, E.Theodoridou, *Synth.Met.*30 (1989) 283-294.
- [6] F. Arifuku, K. Mori, T. Muratani, H. Kurihara, *Bull. Chem. Soc. Jpn.* 65(1992) 1491-1495.
- [7] Z.X. Liang, H.Y.Song,S.J. Liao, *J. Phys. Chem.C*, 115 (2011) 2604-2610.
- [8] N. Kobayashi, T. Osa, *J. Electroanal. Chem.* 157 (1983) 269-281.
- [9] Q. Ma, T. Liu, T. Tang, H. Yin, S. Aia, *Electrochim. Acta* 56 (2011) 8278-8284.

-
- [10] J. Chen, L. Zhao, H. Bai, G. Shi, J. Electroanal. Chem. 657 (2011) 34-38.
- [11] J.-S. Ye, Y. Wen, W.D. Zhang, H.-F. Cui, L.M. Gan, G.Q. Xu, F.-S. Sheu, J. Electroanal. Chem. 562 (2004) 241-246.
- [12] F. Valentini, L. Cristofanelli, M. Carbone, G. Palleschi, Electrochim. Acta, 63 (2012) 37-46.
- [13] G.L. Turdean, I. C. Popescu, A. Curulli, G. Palleschi, Electrochim. Acta 51 (2006) 6435-6441.
- [14] Y. Gao, J. Chen, J. Electroanal. Chem. 578 (2005) 129-136.
- [15] J.B. Xu, T.S. Zhao, L. Zeng, Int.J, Hydrogen Energy, 37 (2012) 15976-15982.
- [16] M. Lefevre, E. Proietti, F. Jaouen, J.P. Dodelet, Science 324 (2009) 71-74.
- [17] R. Jiang, D.T. Tran, J.P. McClure, D. Chu, Electrochim. Acta 75 (2012) 185-190.
- [18] C. Guo, C. Chen, Z. Luo, Int. J. Electrochem. Sci. 8 (2013) 8940-8950.
- [19] P.-B. Xi, Z.-X. Liang, S.-J. Liao, Int. J. Hydrogen Energy, 37 (2012) 4606-4611.
- [20] Q. Yang, Y. Nie, X. Zhu, X. Liu, G. Li, Electrochim. Acta 55 (2009) 276-280.
- [21] M.T. de Groot, M. Merckx, A.H. Wonders, M.T.M. Koper, J. Am. Chem. Soc. 127 (2005) 7579-7586.
- [22] C.-Z. Li, S. Alwarappan, W. Zhang, N. Scafa, X. Zhang, Am. J. Biomed. Sci. 1 (2009) 274-282.
- [23] Y. Lai, Y. Ma, L. Sun, J. Jia, J. Weng, N. Hu, W. Yang, Q. Zhang, Electrochim. Acta 56 (2011) 3153-3158.
- [24] Y.-L. Zhang, H.-X. Shen, J.-L. Sun, C.-X. Zhang, Electrochim. Acta 46 (2001) 2923-2928.
- [25] G.S. Rao, Chem.-Bio. Interact. 80 (1991) 339-347.
- [26] F. Haber, J. Weiss, Proc. R. Soc. London, A. 147 (1934) 332-351.
- [27] R.S. Nicholson, I. Shain, Anal. Chem. 36 (1964) 706-723.
- [28] K. Aoki, K. Tokuda, H. Matsuda, J. Electroanal. Chem. 199 (1986) 69-79.
- [29] R.S. Tieman, L.A. Coury Jr., J.R. Kirchhoff, W.R. Heineman, J. Electroanal. Chem.

-
- 281 (1990) 133-145.
- [30] G. Meyer, M. Savy, *Electrochim. Acta* 22 (1977) 213-215.
- [31] M. Brezina, W. Khalil, J. Koryta, M. Musilova, *J. Electroanal. Chem.* 77 (1977) 237-244.
- [32] H. Zhang, K. Aoki, J. Chen, T. Nishiumi, H. Toda, E. Torita, *Electroanalysis*, 23 (2011) 947-952.
- [33] H. Cao, X. Sun, Y. Zhang, C. Hu, N. Jia, *Anal. Methods*, 4 (2012) 2412-2416.
- [34] I. Inamura, M. Isshiki, T. Araki, *Bull. Chem. Soc. Jpn.* 62 (1989) 2413-2415.
- [35] Y. K.-Konishi, H. Kihara, H. Suzuki, *Eur. J. Biochem.* 170 (1988) 589-595.
- [36] J. Jin, L.S. Li, X. Wang, Y. Li, Y.J. Zhang, X. Chen, Y. Li, T. J. Li, *Langmuir* 15 (1999) 6969-6974.
- [37] A. D. Ryabov, V. N. Goral, L. Gorton, E. Csöregi, *Chem. Eur. J.* 5 (1999) 961-967.
- [38] A.J. Bard, L.R. Faulkner, *Electrochemical Methods: Fundamentals and Applications*, John Wiley & Sons, 2001, pp.505-505.
- [39] K. Aoki, M. Ishida, K. Tokuda, *J. Electroanal. Chem.* 245 (1988) 39-50.
- [40] A.J. Bard, L.R. Faulkner, *Electrochemical Methods: Fundamentals and Applications*, John Wiley & Sons, 2001, pp. 590-591.
- [41] A.M. Toader, E. Volanschi, M.F. Lazarescu, V. Lazarescu, *Electrochim. Acta* 56 (2010) 863-866.
- [42] T. Sagara, S. Takeuchi, K. Kumazaki, N. Nakashima, *J. Electroanal. Chem.* 396 (1995) 525-533.

Figure Captions

Figure 1. Cyclic voltammograms in (a) deaerated and (b) aerated 0.15 M TBAClO₄ + 0.33 mM hemin + DMSO solution, and in (c) aerated 0.15 M TBAClO₄ + DMSO solution for $\nu = 0.1 \text{ V s}^{-1}$ at the GC electrode.

Figure 2. Scan rate dependence of the cathodic peak current at ca. -0.7 V in (a) the deaerated and (b) the aerated 0.15 M TBAClO₄ + 0.40 mM hemin + DMSO solution at the GC electrode.

Figure 3. UV-vis spectra in (a) the deaerated and (c) the aerated DMSO solutions including 0.033 mM hemin + 0.015 M TBAClO₄, and (b) 16 min after -1 V was applied to the Pt mesh electrode in the deaerated solution.

Figure 4. Time variation of the absorbance at (A) 404 nm and (B) 424 nm in the (triangles) aerated and the (circles) deaerated DMSO solutions including 0.033 mM hemin + 0.015 M TBAClO₄ after -1 V was applied to the Pt mesh electrode. The right ordinate is the logarithmic absorbance of the aerated solution at 404 nm.

Figure 5. Variation of the catalytic peak current at -0.7 V with concentration of dioxygen, obtained for $\nu = 0.1 \text{ V s}^{-1}$ at the GC electrode in DMSO solution including 0.4 mM hemin + 0.15 M TBAClO₄.

Figure 6. Dependence of the peak currents at ca. -0.7 V in (open circles) deaerated and (filled circles) aerated solutions on concentrations of hemin at $\nu = 0.1 \text{ V s}^{-1}$.

Figure 7. Time-variations of the peak currents for $\nu = 0.1 \text{ V s}^{-1}$ in (a) 0.09 mM, (b) 0.17 mM, (c) 0.33 mM, and (d) 0 mM hemin including 0.15 M TBAClO₄ + DMSO solutions after air was bubbled into the solutions, where the peak for (a)-(c) was at -0.7 and that for (d) was at -1.2 V.

Figure 8. Scan rate dependence of (circles) the cathodic peak current at ca. -0.7 V in the aerated 0.15 M TBAClO₄ + 0.40 mM hemin + DMSO solution and (triangles) the current subtracted by the diffusion-controlled current of hemin.

Figure 9. Voltammograms in aerated DMSO solution including 0.4 mM hemin + 0.15 M TBAClO₄ at the first (a, c) scan and the 20th (b, d) scan in the two scan domains (c, d: from -0.8 to 0.0 V) and (a, b: from -0.8 to 0.6 V) for $\nu = 0.1 \text{ V s}^{-1}$.

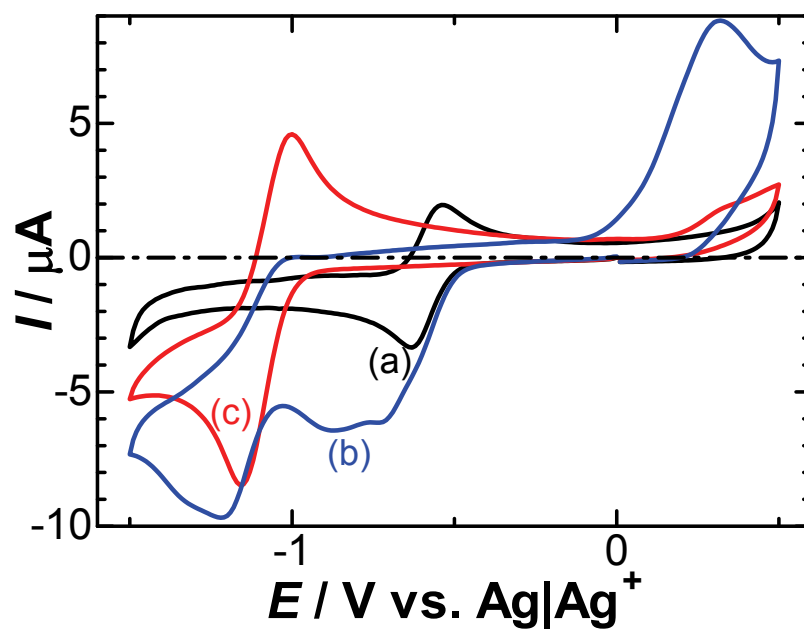


Fig. 1

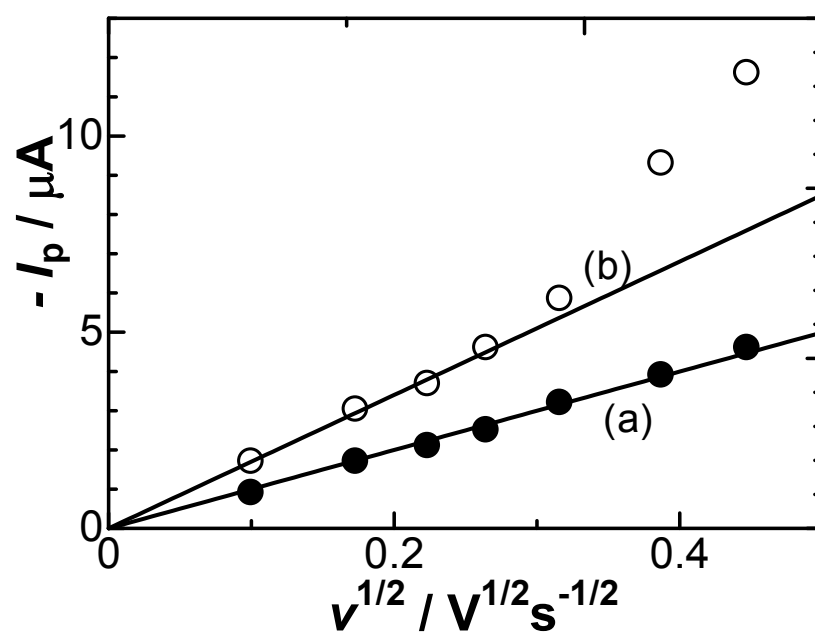


Fig. 2

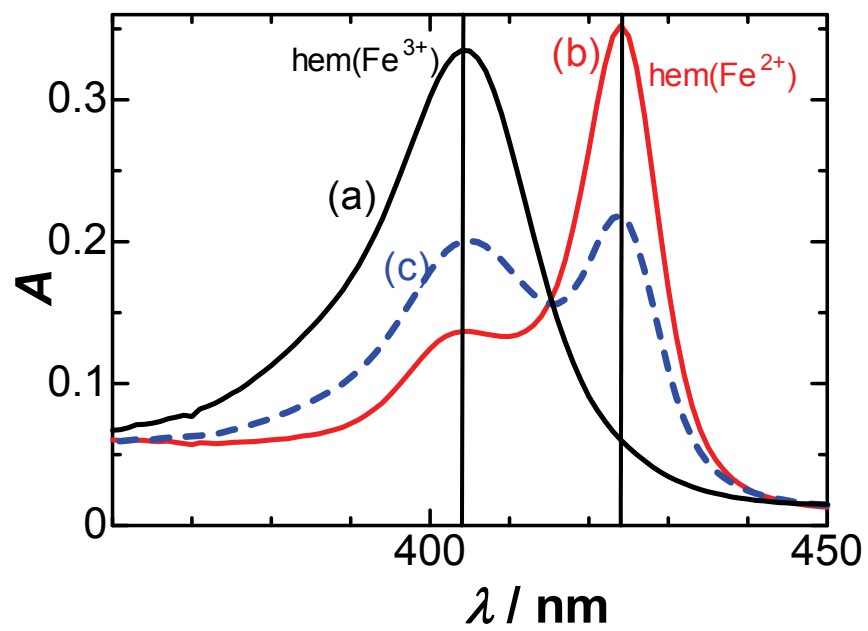


Fig. 3

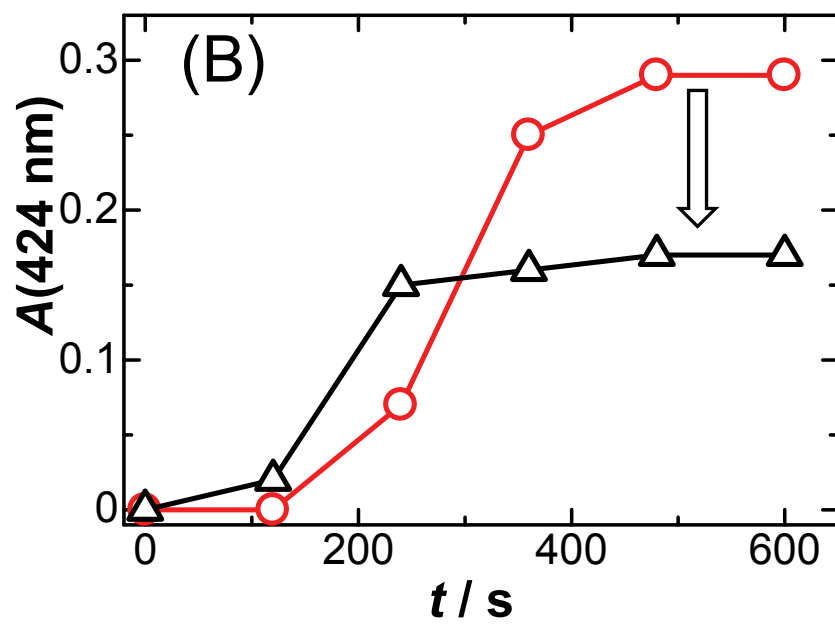
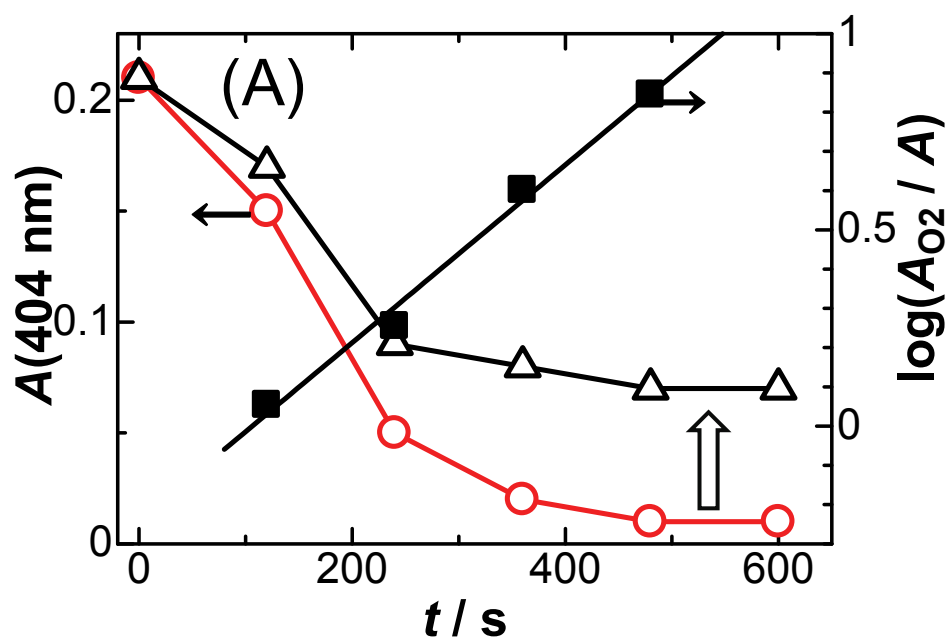


Fig. 4

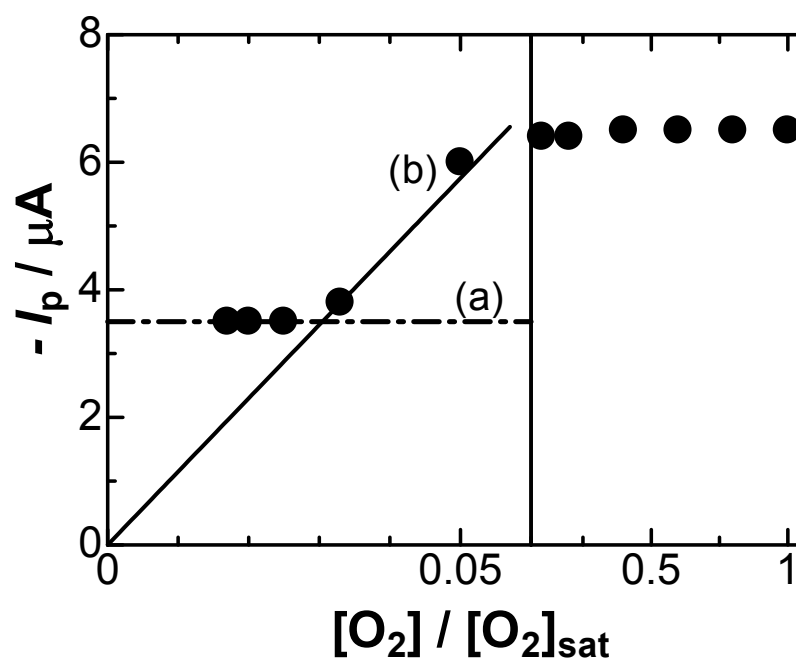


Fig. 5

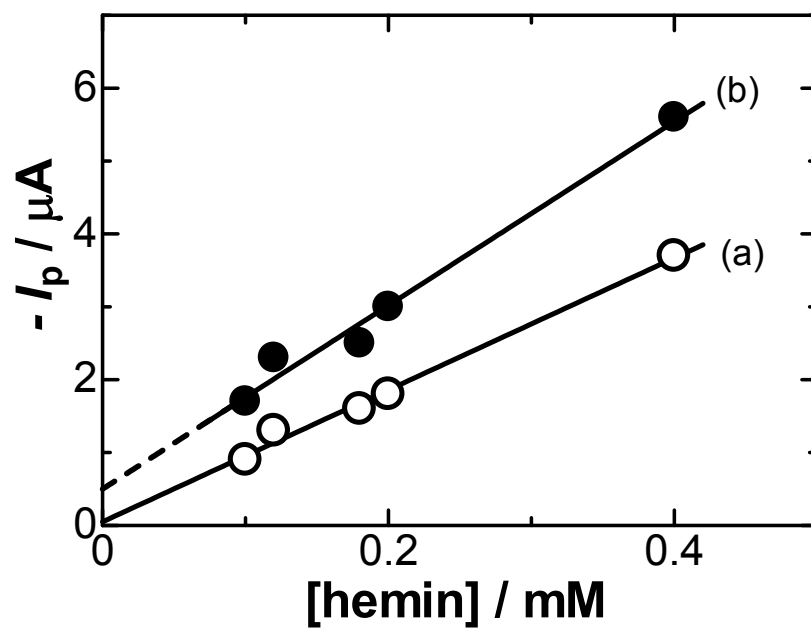


Fig. 6

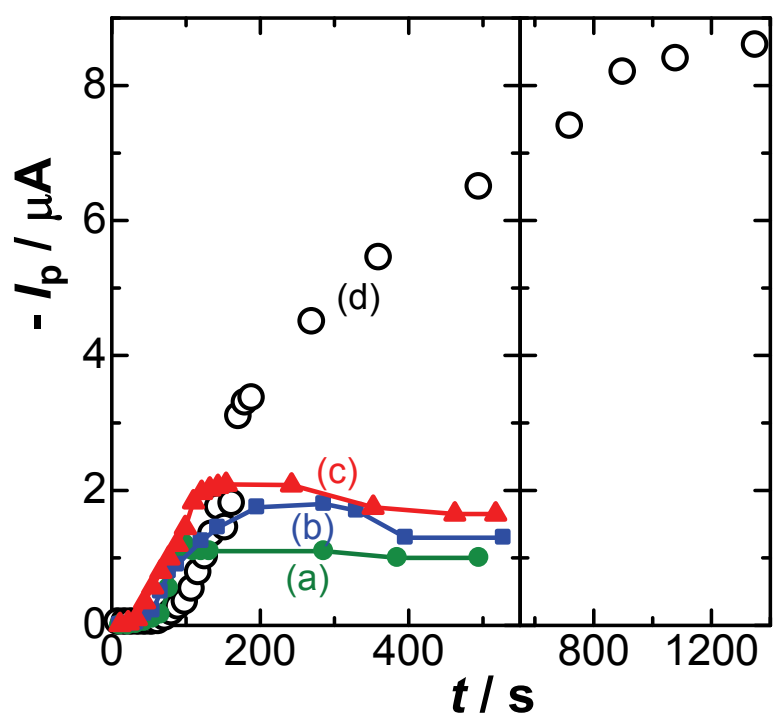


Fig. 7

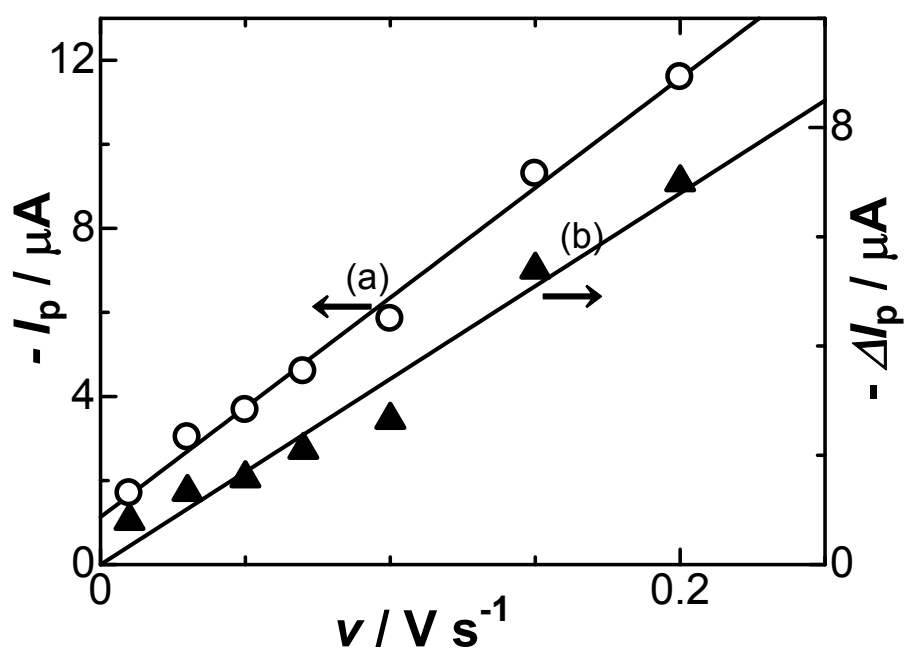


Fig. 8

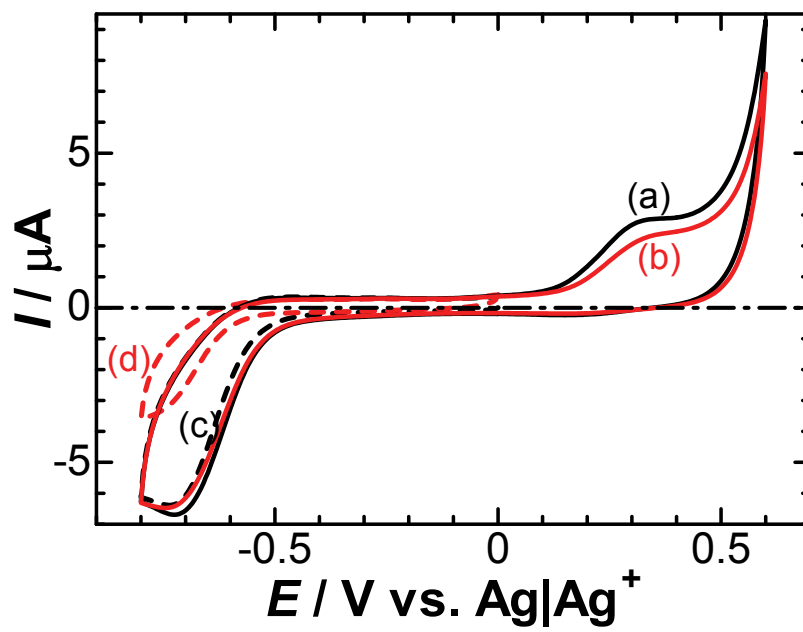


Fig. 9